

Skew scattering by magnetic monopoles and anomalous Hall effect in spin-orbit coupled systems

Jun Mochida^{1,2} and Hiroaki Ishizuka¹

¹*Department of Physics, Tokyo Institute of Technology, Meguro, Tokyo, 152-8551, Japan*

²*Department of Physics, University of Tokyo, 7-3-1 Hongo, Bunkyo-ku, Tokyo 113-0033, Japan*

(Dated: November 21, 2022)

Magnetic textures like skyrmions and domain walls coupled to itinerant electrons give rise to rich transport phenomena such as anomalous Hall effect and nonreciprocal current. An interesting case is when the transport coefficient is related to the global (or topological) property of the magnetic texture, e.g., skyrmion and domain wall numbers. Such phenomena are also interesting from applications, which the transport phenomena are potential probe for electrically detecting magnetic textures in nano-scale devices. Here, we show that an anomalous Hall effect proportional to the net magnetic monopole charge occurs from skew scattering when the magnetic texture couples to itinerant electrons in a non-centrosymmetric system with spin-orbit interaction. This mechanism gives rise to a finite anomalous Hall effect in a ferromagnetic domain wall whose spins rotate in the xy plane, despite no out-of-plane magnetic moment. We also discuss the relation between the magnetic texture contributing to the anomalous Hall effect and the crystal symmetry. The results demonstrate rich features arising from the interplay of spin-orbit interaction and magnetic textures and their potential for detecting various magnetic textures in nanoscale devices.

Noncollinear magnetic textures give rise to numbers of novel phenomena, such as anomalous [1–3] and spin [4, 5] Hall effects, multiferroics [6, 7], and electrical magnetochiral effect [8]. These phenomena are often related to scalar and vector spin chiralities defined by $\mathbf{S}_i \cdot \mathbf{S}_j \times \mathbf{S}_k$ and $\mathbf{S}_i \times \mathbf{S}_j$, respectively. These phenomena were also discussed experimentally. For instance, the anomalous Hall effect (AHE) were studied in transition metal magnets, such as in materials with non-coplanar magnetic order [9] and magnetic skyrmions [10, 11], and the electrical magnetochiral effect in helical magnets [12, 13].

Among various examples, a particularly interesting example is the continuum limit, in which the scalar spin chirality is related to the skyrmion number [1]. In the limit, the Hall conductivity is related to the skyrmion density, as discussed in the perturbation theory [14] and the skew scattering argument [15]. The relation to a topological quantity implies the robustness of the AHE against fluctuations in the spin texture. Such robustness is particularly attractive for applications as it is a potential robust probe for detecting a skyrmion in nano-scale devices, such as race-track memory [16–18]. However, such a relation between the transport coefficient and a quantity characterizing the magnetic texture is rare.

In this work, we study a relation between AHE and the magnetic monopole charge in two-dimensional (2d) systems with spin-orbit interaction (SOI). As a demonstration, we study the anomalous Hall effect in a 2d electron system with Rashba interaction focusing on the skew scattering by magnetic moments. Our calculation shows that, when the magnetic moments lie in the xy plane, the Hall conductivity is proportional to the magnetic monopole charge characterized by the divergence of magnetic moments. We also discuss that the existence of the monopole term is understandable based on the crystal symmetry, which we demonstrate by comparing Rashba and Dresselhaus models. The results unveil a nontrivial relation between the magnetic

charge and transport phenomena, a relation unique to systems with SOI.

AHE generally occurs in magnetic metals with SOI [19]. Pioneering works focus on the AHE in ferromagnets, where the anomalous Hall conductivity follows the magnetization curve [20]. Theoretically, the mechanism of AHE is broadly classified into two groups: the intrinsic mechanism related to Berry curvature [21] and the extrinsic mechanism involving impurity scattering [22, 23]. For the latter, the effect of SOI in the bulk band [24, 25] and magnetic impurity scattering [26–28] were also discussed in addition to the SOI of impurities. In addition to the ferromagnets, recent studies find that non-coplanar magnetic states induce the AHE [1, 2, 14]. The AHE by non-coplanar magnetic order raised interesting questions on the interplay of non-collinear magnetic states and the SOI, which gives rise to rich behaviors in AHE [3, 29–32]. Many works along this direction focus on the intrinsic mechanism, namely the AHE by spin Berry phase.

On the other hand, recently, a skew scattering mechanism by magnetic texture [15] has been proposed [33]. This mechanism potentially gives rise to a larger Hall effect compared to the intrinsic counterpart [5], as observed in recent experiments [34–36]. However, these works discuss the skew scattering in electrons without SOI. We here explore how the SOI affects the AHE by skew scattering, discussing the rich features arising from SOI and their relation to the crystal symmetry.

As a demonstration, we first focus on the Rashba electrons coupled to localized classical XY spins by Kondo

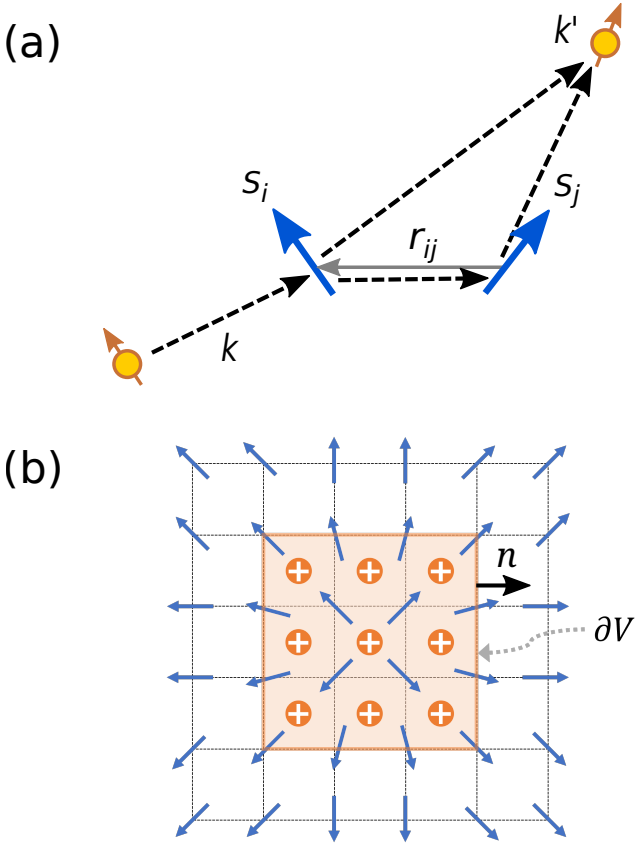


FIG. 1. Schematic of magnetic monopoles and skew scattering. **a.** A schematic of skew scattering involving two spins. Here, \mathbf{r}_{ij} is the vector connecting two spins. **b.** An example of magnetic monopole. V and ∂V denotes the area and its surface, respectively. \mathbf{n} is the normal unit vector on ∂V .

coupling. The Hamiltonian reads

$$H = H_0 + H_K, \quad (1)$$

$$H_0 = \sum_{\mathbf{k}, \alpha, \beta} c_{\mathbf{k}\alpha}^\dagger \left[\left(\frac{\hbar^2 k^2}{2m} - \mu \right) \delta_{\alpha\beta} + \hbar \lambda \hat{z} \cdot \mathbf{k} \times \boldsymbol{\sigma}_{\alpha\beta} \right] c_{\mathbf{k}\beta},$$

$$H_K = -J a^2 \sum_{i, \alpha, \beta} c_{\alpha}^\dagger(\mathbf{r}_i) [\mathbf{S}(\mathbf{r}_i) \cdot \boldsymbol{\sigma}_{\alpha\beta}] c_{\beta}(\mathbf{r}_i),$$

where $c_{\mathbf{k}\alpha}$ ($c_{\mathbf{k}\alpha}^\dagger$) is the annihilation (creation) operator of the electron with momentum $\mathbf{k} = (k_x, k_y)$ and spin α , $c_{\alpha}(\mathbf{r}) = \frac{1}{V} \sum_{\mathbf{k}} e^{i\mathbf{k} \cdot \mathbf{r}} c_{\mathbf{k}\alpha}$ [$c_{\alpha}^\dagger(\mathbf{r}) = \frac{1}{V} \sum_{\mathbf{k}} e^{-i\mathbf{k} \cdot \mathbf{r}} c_{\mathbf{k}\alpha}^\dagger$] is the annihilation (creation) operator of the electron at \mathbf{r} and spin α , $\mathbf{S}(\mathbf{r}_i) = (S^x(\mathbf{r}_i), S^y(\mathbf{r}_i))$ is the classical XY spin at \mathbf{r}_i , and $\boldsymbol{\sigma} = (\sigma^x, \sigma^y, \sigma^z)$ is the vector of Pauli matrices $\sigma^{x,y,z}$. The constant m is the effective mass of the electron, μ is the chemical potential, λ is the spin-orbit coupling, J is the Kondo coupling, a is the lattice constant, and \hbar is the Planck constant. The triple and inner products are $\hat{z} \cdot \mathbf{k} \times \boldsymbol{\sigma} = k_x \sigma^y - k_y \sigma^x$ and $\mathbf{S}(\mathbf{r}) \cdot \boldsymbol{\sigma} = S^x(\mathbf{r}) \sigma^x + S^y(\mathbf{r}) \sigma^y$. The eigenenergy of H_0 reads $\varepsilon_{\mathbf{k}\eta} = \frac{\hbar^2 k^2}{2m} + \eta \hbar \lambda k$ with $\eta = \pm 1$.

	$\mu < 0$	$0 \leq \mu$
σ_1	$\frac{e^2 \tau^2 J^3 a^5}{2\pi^2 \hbar^8} \frac{m^4 \lambda^2 a (\mu + m \lambda^2)}{\sqrt{(\lambda m)^2 + 2m\mu}}$	$\frac{e^2 \tau^2 J^3 a^5}{2\pi^2 \hbar^8} m^3 \lambda a (\mu + m \lambda^2)$
σ_2	$\frac{e^2 \tau^2 J^3 a^5}{4\pi^2 \hbar^7} \frac{m^4 \lambda^3}{\sqrt{(\lambda m)^2 + 2m\mu}}$	$\frac{e^2 \tau^2 J^3 a^5}{4\pi^2 \hbar^7} m^3 \lambda^2$
σ_3	$\frac{e^2 \tau^2 J^3 a^5}{4\pi^2 \hbar^8} \frac{m^4 \lambda^2 a (\mu + m \lambda^2)}{\sqrt{(\lambda m)^2 + 2m\mu}}$	$\frac{e^2 \tau^2 J^3 a^5}{4\pi^2 \hbar^8} m^4 \lambda^3 a$

TABLE I. Coefficients of the Hall conductivities in Eq. (3). The center column is for chemical potential $\mu < 0$ and the right column is for $\mu \geq 0$.

We investigate the Hall effect by evaluating the skew scattering probability using a Born approximation and calculating the Hall conductivity using the scattering probability [See Method for details]. The scattering probability from $\mathbf{k}\eta$ state to $\mathbf{k}'\eta'$ is calculated within second-Born approximation, in which the skew scattering probability $W_{\mathbf{k}\eta \rightarrow \mathbf{k}'\eta'}^- = (W_{\mathbf{k}\eta \rightarrow \mathbf{k}'\eta'} - W_{\mathbf{k}'\eta' \rightarrow \mathbf{k}\eta})/2$ reads

$$W_{\mathbf{k}\eta \rightarrow \mathbf{k}'\eta'}^- = \frac{\pi W_1}{(aL^2)^2} \delta(\varepsilon_{\mathbf{k}\eta} - \varepsilon_{\mathbf{k}'\eta'}) \times \sum_{i,j,l} (\mathbf{S}_l \times \mathbf{r}_{ij}) \cdot (\mathbf{S}_i \times \mathbf{S}_j) \sin \delta\phi, \quad (2)$$

to the leading order in ka , where L is the length of the system, $\delta\phi = a \sin(\hat{z} \cdot \frac{\mathbf{k} \times \mathbf{k}'}{kk'})$ is the scattering angle, and $\mathbf{S}_i = \mathbf{S}(\mathbf{r}_i)$ is the magnetic moment at \mathbf{r}_i . The coefficient W_1 is shown in Tab. III in the Method section. The terms in Eq. (2) is of the order of $(ka)^2$, which is a lower order than the scalar-spin-chirality term in $\mathcal{O}((ka)^3)$ [15]. Hence, these terms potentially gives a larger contribution to the AHE than the scalar-spin-chirality ones, especially when the Fermi surface is small. Moreover, the scattering term in Eq. (2) induce a skew scattering without a finite scalar spin chirality nor magnetic moment perpendicular to the plane, both of which is zero in the XY models.

We calculate the Hall conductivity by the skew scattering using the semiclassical Boltzmann theory [See Method for details]. The conductivity using Eq. (2) reads

$$\sigma_{xy} = -\frac{\sigma_1}{aL^2} \sum_{i,j,l} (\mathbf{S}_l \times \mathbf{r}_{ij}) \cdot (\mathbf{S}_i \times \mathbf{S}_j). \quad (3)$$

Here, the coefficient σ_1 is in Tab. I, where we introduce a phenomenological relaxation rate τ . The coefficients shows different μ dependence reflecting the distinct nature of electron bands above and below $\mu = 0$. A similar result for Heisenberg spin is given in Supplemental Information.

The outer product in the sum of Eq. (3) shows that the scattering by two spins are necessary for a finite σ_{xy} in this system. Note that, due to the zero out-of-plane magnetization, the AHE contributions known in ferromagnets vanishes. However, a finite σ_{xy} appears due to the scattering by multiple spins.

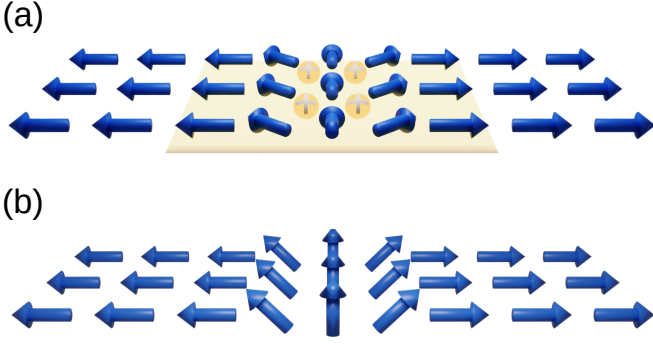


FIG. 2. Schematics of domain walls. (a) A domain wall whose spin rotates in the xy plane. In view of magnetic monopoles, the domain wall corresponds to magnetic monopoles (yellow circles) aligned along the domain wall. (b) A similar argument holds for domain walls with spins rotating out-of-plane.

Focusing on the scattering processes involving two nearest-neighbor spins, i and j , the Hall conductivity reads

$$\sigma_{xy} = \frac{2\sigma_1}{aL^2} \sum_{\langle i,j \rangle} (1 + \mathbf{S}_i \cdot \mathbf{S}_j) [\mathbf{r}_{ij} \cdot (\mathbf{S}_i - \mathbf{S}_j)]. \quad (4)$$

In the continuum limit assuming $\mathbf{S}_i \sim \mathbf{S}_j$, this formula becomes

$$\sigma_{xy} = \frac{4\sigma_1}{aL^2} \int_V d\mathbf{x}^2 \nabla \cdot \mathbf{S}(\mathbf{x}), \quad (5)$$

where $\nabla = (\partial_x, \partial_y)$ and $\nabla \cdot \mathbf{S} = \partial_x S^x(\mathbf{r}) + \partial_y S^y(\mathbf{r})$. Here, we used the gradient expansion and $|\mathbf{S}_i| = 1$. The divergence $\nabla \cdot \mathbf{S}(\mathbf{x})$ defines the magnetic monopole charge of spins, analogous to the definition of electric charge in electromagnetism.

Using the divergence theorem, the above formula reads

$$\sigma_{xy} = \frac{4\sigma_1}{aL^2} \int_{\partial V} \mathbf{n}(\mathbf{x}) \cdot \mathbf{S}(\mathbf{x}) d\ell, \quad (6)$$

as in the Gauss' theorem in electromagnetism. Here, the integral is taken over the boundary of the system ∂V , where $\mathbf{n}(\mathbf{x})$ is the unit vector perpendicular to the boundary [Fig. 1(b)]. Hence, the anomalous Hall conductivity is related to the net magnetic charge, not to the fine details of the spin structure.

As an example of the magnetic monopole, we first discuss the vortex in Fig. 1(b). The spin configuration reads $\mathbf{S}(\mathbf{r}) = (\cos(\phi), \sin(\phi), 0)$, where ϕ is the azimuth. The Hall conductivity reads

$$\sigma_{xy} = \frac{8\pi\sigma_1}{aL}. \quad (7)$$

A finite Hall effect by the magnetic monopole implies that the monopoles are electrically detectable using the Hall effect, similar to the detection of skyrmions using anomalous Hall effect.

A more familiar example of the magnetic monopole is the domain walls of ferromagnets [Fig. 2]. The domain

	π	C_2^z	C_2^x	C_2^y	M_z	M_x	M_y	C_3^z	C_4^z	C_6^z
$\nabla \cdot \mathbf{S}_\perp$	0	-	0	0	0	-	-	-	-	-
$(\nabla \times \mathbf{S}_\perp)^z$	0	-	-	-	0	0	0	-	0	-
$\sigma_{\text{Dressel}}^1$	0	-	-	-	0	0	0	0	-	0
$\sigma_{\text{Dressel}}^2$	0	-	-	-	0	0	0	-	-	-
Rashba	\times	\circ	\times	\times	\times	\circ	\circ	\circ	\circ	\circ
Dresselhaus	\times	\circ	\circ	\circ	\times	\times	\times	\times	\times	\times

TABLE II. Symmetries of AHE and SOI. In the table, it is written as "0" if each conductivity in the phenomenological AHE formula vanishes under each symmetry. $\nabla \cdot \mathbf{S}_\perp$ and $(\nabla \times \mathbf{S}_\perp)^z$ are the Hall current proportional to the divergence and rotation of the magnetic texture, respectively. $\sigma_{\text{Dressel}}^1$ and $\sigma_{\text{Dressel}}^2$ are respectively the first and second terms in Eq. (9).

wall is a boundary between the two ferromagnetic domains whose magnetization points along the opposite directions [Fig. 2]. For the XY spins, the spins rotate within the xy plane [Fig. 2(a)]. In view of magnetic monopole, this domain wall corresponds to a line of magnetic charges. Mathematically, the correspondence is explicitly shown by applying the Gauss' law to the region surrounding the wall [yellow region in Fig. 2(a)]. Note that the y component of spins does not contribute to the monopole charge because it is uniform along the y axis. Using Eq. (6), the Hall conductivity reads

$$\sigma_{xy} = \frac{8\sigma_1}{aL}. \quad (8)$$

Note that the conductivity scales L^{-1} to the system size L . However, it gives an observable consequence if σ_1 is sufficiently large.

To examine the typical magnitude of the response, we estimate the Hall conductivity using a set of values for Rashba electron known in the experiment [37]: $m = 10^{-30}$ kg, $\mu = 0.19$ eV, $a = 4.3$ Å, and $\hbar\lambda = 3.8$ eVÅ. Assuming the Kondo coupling $J = 0.1$ eV, the Hall conductivity becomes $\sigma_{xy} \sim 10^4 \Omega^{-1}\text{cm}^{-1}$ for a domain wall in $L = 1$ μm in size device. The number is sufficiently large for the observation in experiments [19]. The Hall conductivity is determined solely by the direction of magnetic moments in the two adjacent domains or the magnetization at the boundary of the device [the boundary of the shaded region in Fig. 2(a)], as discussed above. In other words, the detail of the domain wall structure does not affect the result. The robustness against the fine structure of domain wall implies that this AHE is potentially a good probe of domain walls.

The reason we find $\nabla \cdot \mathbf{S}$ term in the Rashba model can be understood from the symmetry viewpoint. The AHE by magnetic monopole is phenomenologically described by a formula $J_y = \sigma \int \nabla \cdot \mathbf{S}_\perp(\mathbf{r}) dr^2 E_x$. For example, when the inversion symmetry exists in the system, the symmetry operation transforms $\mathbf{S}_\perp(\mathbf{r}) \rightarrow \mathbf{S}_\perp(-\mathbf{r})$, $J_y \rightarrow -J_y$, and $E_x \rightarrow -E_x$. Hence, the phenomenological formula becomes $J_y = -\sigma \int \nabla \cdot \mathbf{S}_\perp(\mathbf{r}) dr^2 E_x$. Thus, $\sigma = -\sigma$ for the system with inversion symmetry, implying that the

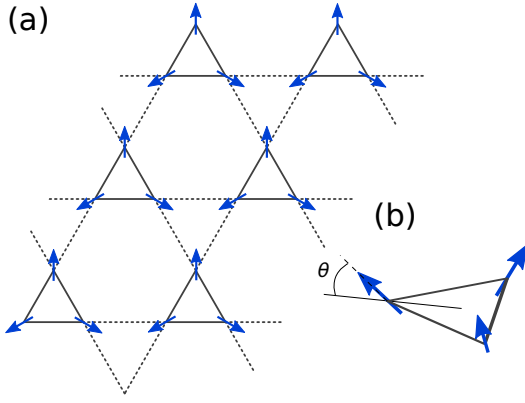


FIG. 3. Schematic of (a) breathing kagomé lattice. The bond lengths for upward and downward triangle are different. (b) The out-of-plane canting angle is defined by the angle between the spin and the kagomé plane.

AHE proportional to $\nabla \cdot \mathbf{S}_\perp$ vanishes. Similarly, the mirror operation about the z axis, $M_z: x, y \rightarrow x, y$ and $z \rightarrow -z$, gives $\sigma = -\sigma$, again implying the Hall effect is prohibited. The top half of Tab. II shows the symmetry requirements, where 0 denotes the vanishing Hall conductivity. The lower half of the table shows the symmetry of Rashba and Dresselhaus models, where the \times in the table denotes the symmetry do not exist in the model.

Reflecting the symmetry property, the $\nabla \cdot \mathbf{S}$ term is allowed in Rashba model whereas the Hall effect related to other form of spin structure is possible in the Dresselhaus model. Applying the same method to Dresselhaus model, we find that the Hall conductivity reads

$$\sigma_{xy} = \frac{2\sigma_1}{aL^2} \int dx^2 [S^x(\mathbf{S} \times \partial_x \mathbf{S})_z - S^y(\mathbf{S} \times \partial_y \mathbf{S})_z] - \frac{2\sigma_1}{aL^2} \int dx^2 [\partial_x S^y + \partial_y S^x] \quad (9)$$

in the continuum limit [See Supplementary Information for details]. Here, we find vanishing the $\nabla \cdot \mathbf{S}$ term as expected from Tab. II. As demonstrated by the two models, the form of spin textures reflected to AHE is understandable from the crystal symmetry.

We next look at the effect of the lattice distortion, in particular the formation of clusters. In some materials, the lattice distortion forms a cluster of spins such as in trimerized triangular lattice [36] and in breathing kagomé [38, 39] and pyrochlore [40, 41] magnets. As a concrete example, we consider a breathing kagomé lattice with canted 120° spin configuration as in Fig. 3(a). By extending Eq. (3) to the spins with nonzero S^z , the Hall conductivity reads

$$\sigma_{xy} = 12\sigma_1\delta \cos\theta(1 + 3\sin^2\theta) + 24\sqrt{3}\sigma_2\sin^3\theta - 48\sigma_3\delta \cos\theta\sin^2\theta, \quad (10)$$

where θ is the out-of-plane canting angle, and the bond length of the upward (downward) triangle is $(\frac{1}{2} + \delta)a$ [$(\frac{1}{2} - \delta)a$] [Fig. 3(b)]. When $\theta = 0$, i.e., for the coplanar 120°

order, the conductivity becomes $\sigma_{xy} = 12\sigma_1\delta$. Unlike the uniform case discussed in the previous sections, the Hall conductivity in the distorted kagomé lattice remains finite in the bulk limit.

In view of the magnetic monopole, the 120° order is a pair of monopole and anti-monopole (the monopole with the opposite charge). Hence, the total monopole charge is zero which is consistent with the zero Hall conductivity at $\delta = 0$. In presence of the breathing, however, the breathing breaks the cancellation between monopole and anti-monopole contributions, giving a finite Hall effect. The result shows that the monopole-related Hall effect also occurs in the bulk when the lattice distortion, such as breathing, exists in the lattice.

In this work, we systematically study the skew scattering by multiple spins in systems with strong SOI. Beside the skew scattering term similar to one discussed by Kondo [26], we find two terms contributing to the skew scattering. These terms appear in the order of $(ka)^2$, in contrast to the $(ka)^3$ for the chirality-related AHE [15]. Hence, the novel terms potentially give a larger contribution to the AHE in magnetic semiconductors where ka is small due to the small Fermi surface, such as semiconductors described by Rashba and Dresselhaus models. A particularly interesting term is that proportional to $(1 + \mathbf{S}_i \cdot \mathbf{S}_j)[\mathbf{r}_{ij} \cdot (\mathbf{S}_i - \mathbf{S}_j)]$, which gives a skew scattering proportional to the magnetic monopoles in the continuous limit, $\nabla \cdot \mathbf{S}(\mathbf{r})$. We find that this is the only term that contributes to AHE when the spins lie in the xy plane, e.g., for magnetic metals with the easy-plane anisotropy. The $\nabla \cdot \mathbf{S}(\mathbf{r})$ term gives rise to AHE in the presence of a vortex-like defect or domain walls, or in a material with breathing-type distortion.

The Hall effect proportional to $\nabla \cdot \mathbf{S}(\mathbf{r})$ contributes to the AHE in the presence of a vortex-like structures in Fig. 1(b) and in domain walls [Fig. 2(a)]. Importantly, the Hall conductivity depends only on the spin configuration of the bulk surrounding the vortex or the domain wall, and not to the fine details of the spin structure. Such robustness to the detail is also interesting from application viewpoint, especially as the local probe for detecting magnetic structures which is a key technology in racetrack memory (Ref. [16–18]).

In the last, we note that a recent work studying the effect of SOI on the AHE by non-collinear magnetic states finds vanishing contribution from the SOI [31]. This work focuses the intrinsic AHE from the Berry phase viewpoint, in which they find only two relevant contributions: the conventional AHE by ferromagnetic moment and the chirality-related AHE. In contrast, our study finds the skew scattering by magnetic moments is strongly affected by the SOI, which gives rise to rich features not seen in the systems without SOI.

	$\mu < 0$	$0 \leq \mu$
W_1	$(k_{\xi'} + k_{\xi}) \frac{J^3 a^5}{2\hbar^3} \frac{m^2 \lambda}{\sqrt{m^2 \lambda^2 + 2m\mu}}$	$-(\eta k' + \eta' k) \frac{J^3 a^5}{2\hbar^3} m$
W_2	$-\frac{J^3 a^5}{\hbar^3} \frac{m^2 \lambda}{\sqrt{m^2 \lambda^2 + 2m\mu}}$	$-\eta \eta' \frac{J^3 a^5}{\hbar^3} m$
W_3	$\frac{J^3 a^5}{2\hbar^4} \frac{m^3 (\mu + m\lambda^2)}{\sqrt{m^2 \lambda^2 + 2m\mu}}$	$\eta \eta' \frac{J^3 a^5 \lambda}{2\hbar^4} m^2$
W_4	$(k_{\xi'} - k_{\xi}) \frac{J^3 a^5}{2\hbar^3} \frac{m^2 \lambda}{\sqrt{m^2 \lambda^2 + 2m\mu}}$	$(\eta' k - \eta k') \frac{J^3 a^5}{2\hbar^3} m$

TABLE III. Coefficients of the skew scattering in the Rashba electron in Eqs. (2) and (16). The left column is for chemical potential $\mu < 0$ and the right column is for $\mu \geq 0$.

METHOD

Here we provide the details of the scattering and Boltzmann theory. We investigate the scattering rate of the magnetic scattering processes using a second Born approximation. The rate of scattering an electron with momentum \mathbf{k} and spin α to that of \mathbf{k}' and β is given as

$$W_{\mathbf{k}\alpha \rightarrow \mathbf{k}'\beta} = \frac{2\pi}{\hbar} \left| N_{\mathbf{k}\alpha, \mathbf{k}'\beta}^{(1)} + N_{\mathbf{k}\alpha, \mathbf{k}'\beta}^{(2)} \right|^2 \delta(\varepsilon_{\mathbf{k}\alpha} - \varepsilon_{\mathbf{k}'\beta}), \quad (11)$$

where $N_{\mathbf{k}\alpha, \mathbf{k}'\beta}^{(1)}$ and $N_{\mathbf{k}\alpha, \mathbf{k}'\beta}^{(2)}$ are the first and second-order scattering amplitudes respectively. In our work, we treat the Kondo Hamiltonian H_K as a perturbation to the non-perturbative Hamiltonian H_0 in Eq. (1). Then, scattering amplitudes are given by

$$N_{\mathbf{k}\alpha, \mathbf{k}'\beta}^{(1)} = \langle \mathbf{k}\alpha | H_K | \mathbf{k}'\beta \rangle, \quad (12)$$

$$N_{\mathbf{k}\alpha, \mathbf{k}'\beta}^{(2)} = \sum_{\mathbf{p}, \eta} \frac{\langle \mathbf{k}\alpha | H_K | \mathbf{p}\eta \rangle \langle \mathbf{p}\eta | H_K | \mathbf{k}'\beta \rangle}{\varepsilon_{\mathbf{k}\alpha} - \varepsilon_{\mathbf{p}\eta} - i0}, \quad (13)$$

where $|\mathbf{k}\alpha\rangle$ denotes an eigenstate of H_0 and $\varepsilon_{\mathbf{k}\alpha}$ is an eigenenergy of that. Since the band structure of the system with the SOI is qualitatively different between $\varepsilon_{\mathbf{k}\alpha} > 0$ and $\varepsilon_{\mathbf{k}\alpha} < 0$, physical properties such as skew scattering and transport coefficients change qualitatively through the sign of the chemical potential. As the scattering process is elastic, $\varepsilon_{\mathbf{k}\alpha} = \varepsilon_{\mathbf{k}'\beta}$, we can express the magnitude of the momentum k as a function of the chemical potential μ and the band index η ,

$$k_{\xi}(\mu, \eta) = \frac{-\eta \lambda m + \xi \sqrt{\lambda^2 m^2 + 2m\mu}}{\hbar}, \quad (14)$$

where $\xi, \eta = \pm 1$. For $\mu \geq 0$, only $\xi = +1$ appears while only $\eta = -1$ appears in $\mu < 0$. To avoid redundancy, the notation as $k_{\xi} = k_{\xi}(\mu < 0, \eta = -1)$, $k = k_{\xi=+1}(\mu \geq 0, \eta)$ and $k' = k_{\xi=+1}(\mu \geq 0, \eta')$ are used in this section.

To examine the effect of the magnetic scattering on the AHE, we mainly focus on the antisymmetric part of the

scattering rate defined as

$$\begin{aligned} W_{\mathbf{k}\alpha \rightarrow \mathbf{k}'\beta}^- &= \frac{W_{\mathbf{k}\alpha \rightarrow \mathbf{k}'\beta} - W_{\mathbf{k}'\beta \rightarrow \mathbf{k}\alpha}}{2} \\ &= \frac{4\pi^2}{\hbar} \sum_{\mathbf{p}, \eta} \Im[\langle \mathbf{k}'\beta | H_K | \mathbf{k}\alpha \rangle \langle \mathbf{k}\alpha | H_K | \mathbf{p}\eta \rangle \langle \mathbf{p}\eta | H_K | \mathbf{k}'\beta \rangle] \\ &\quad \times \delta(\varepsilon_{\mathbf{k}\alpha} - \varepsilon_{\mathbf{k}'\beta}) \delta(\varepsilon_{\mathbf{p}\eta} - \varepsilon_{\mathbf{k}\alpha}) \delta(\varepsilon_{\mathbf{p}\eta} - \varepsilon_{\mathbf{k}'\beta}), \quad (15) \end{aligned}$$

where $\delta(x)$ is the Dirac delta function. We derived the second line of Eq. (15) from Eq. (11). Equation (15) for the Rashba system reads

$$\begin{aligned} W_{\mathbf{k}\eta \rightarrow \mathbf{k}'\eta'}^- &= \pi \delta(\varepsilon_{k\eta} - \varepsilon_{k'\eta'}) \\ &\cdot \sum_{i,j,l} \left[\frac{W_1}{(aL^2)^2} (\mathbf{S}_l \times \mathbf{r}_{ij}) \cdot (\mathbf{S}_i \times \mathbf{S}_j) - \frac{W_2}{(L^2)^2} S_l^z (\mathbf{S}_i \cdot \mathbf{S}_j) \right. \\ &\quad \left. + \frac{W_3}{(aL^2)^2} S_l^z (\hat{\mathbf{z}} \times \mathbf{r}_{ij}) \cdot (\mathbf{S}_i \times \mathbf{S}_j) \right] \sin \delta\phi \\ &+ \delta(\varepsilon_{k\eta} - \varepsilon_{k'\eta'}) \frac{W_4}{(aL^2)^2} \sum_{i,j,l} (\mathbf{S}_i \cdot \mathbf{S}_j) (\hat{\mathbf{z}} \cdot \mathbf{r}_{il} \times \mathbf{S}_l) \cos \delta\phi, \quad (16) \end{aligned}$$

for Heisenberg spins \mathbf{S}_i ; the $S_i^z = 0$ case corresponds to the XY spin case. Here, we neglect higher order terms of $\mathcal{O}((ka)^3)$, $\mathcal{O}(J^4)$, and assume $2m\lambda/\hbar$ is same order of k . The skew terms are taken averaged over the mean angle $\bar{\phi} = (\phi_k + \phi_{k'})/2$, where ϕ_k is the direction of the electron momentum \mathbf{k} . Then, Eq. (16) only depends on the scattering angle $\delta\phi = \phi_k - \phi_{k'}$. Each coefficient W_i is summarized in in Tab. III. As mentioned in the main text, all terms in Eq. (16) are different from scalar-spin-chirality term that appears without the SOI systems on the order of $\mathcal{O}((ka)^3)$.

Next, we evaluate the Hall conductivity which arises from the skew scattering in Eq. (16) within the semi-classical Boltzmann theory. In the presence of the uniform static electric field \mathbf{E} , the Boltzmann equation reads

$$e\mathbf{E} \cdot \mathbf{v}_{\mathbf{k}\eta} f_0'(\mu) = \frac{g_{\mathbf{k}\eta}}{\tau} - \frac{V}{(2\pi)^2} \sum_{\eta} \int d^2k W_{\mathbf{k}'\eta' \rightarrow \mathbf{k}\eta}^- g_{\mathbf{k}'\eta'}, \quad (17)$$

where $\mathbf{v}_{\mathbf{k}\eta} = \nabla_{\mathbf{k}} \varepsilon_{\mathbf{k}\eta} / \hbar$ is the velocity of the electron in the momentum \mathbf{k} , and $f_0(\varepsilon)$ is the Fermi-Dirac distribution with its energy derivative $f_0'(\varepsilon)$. We assume that the electron distribution is expanded as $f_{\mathbf{k}\eta} = f_0(\varepsilon_{\mathbf{k}\eta}) + g_{\mathbf{k}\eta}$ and the displacement from the equilibrium distribution $g_{\mathbf{k}\eta}$ is order E . For the scattering terms in the right-hand side of Eq. (17), the symmetric part of the scattering rate $W_{\mathbf{k}\eta \rightarrow \mathbf{k}'\eta'}^+ = (W_{\mathbf{k}\eta \rightarrow \mathbf{k}'\eta'} + W_{\mathbf{k}'\eta' \rightarrow \mathbf{k}\eta})/2$ is taken into account the relaxation time approximation with relaxation time τ .

Equation (17) is analytically solvable for W^- [15]. In order to evaluate the displacement $g_{\mathbf{k}\eta}$, we define a parameter $\mathbf{P}_{\eta}(\mu)$ related to the integral of $g_{\mathbf{k}\eta}$ with respect to the

angle as

$$\mathbf{P}_\eta(\mu) = \int_0^{2\pi} d\phi_k \hat{k} g_{\mathbf{k}\eta}, \quad (18)$$

where \hat{k} is the unit vector along \mathbf{k} . Using \mathbf{P}_η , we rewrite the Boltzmann equation as

$$g_\eta = e\tau \mathbf{E} \cdot \mathbf{v}_\mathbf{k} f'_0(\varepsilon) + \tau \tilde{W}^- \sum_{\eta'} V^{\eta\eta'}(\mu) \hat{z} \cdot \hat{k} \times \mathbf{P}_{\eta'}(\mu), \quad (19)$$

where \tilde{W}^- and $V^{\eta\eta'}$ are the coefficients from Eq. (16) as follows,

$$\tilde{W}^- = \frac{1}{4\pi v(\mu)} \frac{J^3 a^6}{L^2 \hbar^4} m, \quad (20)$$

$$V^{\eta\eta'}(\mu) = \begin{cases} \frac{\lambda k_{\eta'}}{v(\mu)} \left[-\frac{1}{2}(k_{\eta'} + k_\eta) \sum_{ijl} (\mathbf{S}_l \times \mathbf{r}_{ij}) \cdot (\mathbf{S}_i \times \mathbf{S}_j) + \sum_{ijl} S_l^z (\mathbf{S}_i \cdot \mathbf{S}_j) - \frac{\mu + m\lambda^2}{\hbar\lambda} \sum_{ijl} S_l^z (\hat{z} \times \mathbf{r}_{ij}) \cdot (\mathbf{S}_i \times \mathbf{S}_j) \right] & (\mu < 0), \\ k' \left[\frac{1}{2}(\eta k' + \eta' k) \sum_{ijl} (\mathbf{S}_l \times \mathbf{r}_{ij}) \cdot (\mathbf{S}_i \times \mathbf{S}_j) + \eta\eta' \sum_{ijl} S_l^z (\mathbf{S}_i \cdot \mathbf{S}_j) - \eta\eta' \frac{m\lambda}{\hbar} \sum_{ijl} S_l^z (\hat{z} \times \mathbf{r}_{ij}) \cdot (\mathbf{S}_i \times \mathbf{S}_j) \right] & (\mu \geq 0), \end{cases} \quad (21)$$

where $v(\mu) = |\mathbf{v}_\mathbf{k}|$. By multiplying \hat{k} to the both sides of Eq. (19) and integrating over ϕ_k , we get the following self-consistent equation respect to \mathbf{P}_η :

$$\mathbf{P}_\eta = e\tau\pi v \mathbf{E} f'_0(\mu) + \pi\tau \tilde{W}^- \sum_{\eta'} V^{\eta\eta'} \mathbf{P}_{\eta'}(\mu) \times \hat{z}. \quad (22)$$

Eq. (22) is a linear equation of \mathbf{P}_η and can be solved analytically. TO the leading order of J^3 , \mathbf{P}_η is expressed as

$$\mathbf{P}_\eta(\mu) = e\tau\pi v f'_0(\mu) (\mathbf{E} - \pi\tau \tilde{W}^- \hat{z} \times \mathbf{E} \sum_{\eta'} V^{\eta\eta'}). \quad (23)$$

Finally, the Hall conductivity is calculated using the current formula

$$\mathbf{j} = \frac{-e}{(2\pi)^2} \sum_{\eta} \int d^2k \mathbf{v}_{\mathbf{k}\eta} g_{\mathbf{k}\eta}, \quad (24)$$

by substituting Eq. (23) for Eq. (19). The results for the XY spins are given in Eq. (3), and for the Heisenberg spins in the Supplementary Information.

ACKNOWLEDGEMENT

We are thankful to Y. Niimi and K. Masuki for discussions. This work is supported by JSPS KAKENHI (Grant Number JP19K14649).

[1] Ye, J. *et al.* Berry phase theory of the anomalous Hall effect: application to colossal magnetoresistance manganites. *Phys. Rev. Lett.* **83**, 3737 (1999).

- [2] Ohgushi, K., Murakami, S. & Nagaosa, N. Spin anisotropy and quantum Hall effect in the kagomé lattice: chiral spin state based on a ferromagnet. *Phys. Rev. B* **62**, R6065 (2000).
- [3] Chen, H., Niu, Q. & MacDonald, A. H. Anomalous Hall effect arising from noncollinear antiferromagnetism *Phys. Rev. Lett.* **112**, 017205 (2014).
- [4] Ishizuka, H. & Motome, Y. Spontaneous spacial inversion symmetry breaking and spin Hall effect in a spin-ice double-exchange model on a pyrochlore lattice. *Phys. Rev. B* **88**, 100402(R) (2013).
- [5] Ishizuka, H. & Nagaosa, N. Large anomalous Hall effect and spin Hall effect by spin-cluster scattering in the strong-coupling limit. *Phys. Rev. B* **103**, 235148 (2021).
- [6] Katsura, H., Nagaosa, N. & Balatsky, A. V. Spin current and magnetoelectric effect in noncollinear magnets. *Phys. Rev. Lett.* **95**, 057205 (2005).
- [7] Bulaevskii, L. N., Batista, C. D., Mostovoy, M. V. & Khomskii, D. I. Electronic orbital currents and polarization in Mott insulators. *Phys. Rev. B* **78**, 024402 (2008).
- [8] Ishizuka, H. & Nagaosa, N. Anomalous electrical magnetochiral effect by chiral spin correlation. *Nat. Commun.* **11**, 2986 (2020).
- [9] Taguchi, Y., Oohara, Y., Yoshizawa, H., Nagaosa, N. & Tokura, Y. Spin chirality, Berry phase, and anomalous Hall effect in a frustrated ferromagnet. *Science* **291**, 2573 (2001).
- [10] Neubauer, A. *et al.* Topological Hall effect in the A phase of MnSi. *Phys. Rev. Lett.* **102**, 186602 (2009).
- [11] Kurumaji, T., Nakajima, T., Hirschberger, M., Kikkawa, A., Yamasaki, Y., Sagayama, H., Nakao, H., Taguchi, Y., Arima, T. & Tokura, Y. Skyrmion lattice with a giant topological Hall effect in a frustrated triangular-lattice magnet. *Science* **365**, 914 (2019).
- [12] Yokouchi, T. *et al.* Electrical magnetochiral effect induced by chiral spin fluctuations. *Nat. Commun.* **8**, 866 (2017).

- [13] Aoki, R., Kousaka, Y. & Togawa, Y. Anomalous nonreciprocal electrical transport on chiral magnetic order. *Phys. Rev. Lett.* **122**, 057206 (2019).
- [14] Onoda, M., Tatara, G. & Nagaosa, N. Anomalous Hall Effect and Skyrmion Number in Real and Momentum Spaces. *J. Phys. Soc. Jpn.* **73**, 2624 (2004).
- [15] Ishizuka, H. & Nagaosa, N. Spin chirality induced skew scattering and anomalous Hall effect in chiral magnets. *Sci. Adv.* **4**, eaap9962 (2018).
- [16] Fert, A., Cros, V. & Sampaio, J. Skyrmions on the track. *Nat. Nanotech.* **8**, 152 (2013).
- [17] Tomasello, R., Martinez, E., Zivieri, R., Torres, L., Carpentieri, M. & Finocchio, G. A strategy for the design of skyrmion racetrack memories. *Sci. Rep.* **4**, 6784 (2014).
- [18] Maccariello, D., Legrand, W., Reyren, N., Garcia, K., Bouzehouane, K., Collin, S., Cros, V. & Fert, A. Electrical detection of single magnetic skyrmions in metallic multilayers at room temperature. *Nat. Nanotech.* **13**, 233 (2018).
- [19] Nagaosa, N., Sinova, J., Onoda, S., MacDonald, A. H. & Ong, N. P. Anomalous Hall effect. *Rev. Mod. Phys.* **82**, 1539 (2010).
- [20] Hall, E. H. XVIII. On the “Rotational Coefficient” in nickel and cobalt. *Phil. Mag.* **12**, 157 (1881).
- [21] Karplus, R. & Luttinger, J. M. Hall Effect in Ferromagnetics. *Phys. Rev.* **95**, 1154 (1954).
- [22] Smit, J. The spontaneous hall effect in ferromagnetics I. *Physica* **21**, 877 (1955).
- [23] Berger, L. Side-Jump Mechanism for the Hall Effect of Ferromagnets. *Phys. Rev. B* **2**, 4559 (1970).
- [24] Adams, E. & Blount, E. Energy bands in the presence of an external force field—II: Anomalous velocities. *J. Phys. Chem. Sol.* **10**, 286 (1959).
- [25] Ishizuka, H. & Nagaosa, N. Noncommutative quantum mechanics and skew scattering in ferromagnetic metals. *Phys. Rev. B* **96**, 165202 (2017).
- [26] Kondo, J. Anomalous Hall effect and magnetoresistance of ferromagnetic metals. *Prog. Theor. Phys.* **27**, 772–792 (1962).
- [27] Fert, A. & Levy, P. M. Theory of the Hall effect in heavy-fermion compounds. *Phys. Rev. B* **36**, 1907 (1987).
- [28] Yamada, K., Kontani, H., Kohno, H. & Inagaki, S. Anomalous Hall Coefficient in Heavy Electron Systems. *Prog. Theor. Phys.* **89**, 1155 (1993).
- [29] Lux, F. R., Freimuth, F., Blügel, S. & Mokrousov, Y. Chiral Hall Effect in Noncollinear Magnets from a Cyclic Cohomology Approach. *Phys. Rev. Lett.* **124**, 096602 (2020).
- [30] Zhang, S.-S., Ishizuka, H., Zhang, H., Halász, G. B. & Batista, C. D. Real-space Berry curvature of itinerant electron systems with spin-orbit interaction. *Phys. Rev. B* **101**, 024420 (2020).
- [31] Yokoyama, T. Absence of Hall effect due to Berry curvature in phase space. *Sci. Rep.* **11**, 12065 (2021).
- [32] Yamaguchi, T. & Yamakage, A. Theory of Magnetic-Texture-Induced Anomalous Hall Effect on the Surface of Topological Insulators. *J. Phys. Soc. Jpn.* **90**, 063703 (2021).
- [33] Kanazawa, N., Onose, Y., Arima, T., Okuyama, D., Ohoyama, K., Wakimoto, S., Kakurai, K., Ishiwata, S., Tokura, Y. Large topological Hall effect in a short-period helimagnet MnGe. *Phys. Rev. Lett.* **106**, 156603 (2011).
- [34] Yang, S.-Y., Wang, Y., Ortiz, B. R., Liu, D., Gayles, J., Derunova, E., Gonzalez-Hernandez, R., Smejkal, L., Chen, Y., Parkin, S. S. P., Wilson, S. D., Toberer, E. S., McQueen, T., Mazhar N. Ali, M. N. Giant, unconventional anomalous Hall effect in the metallic frustrated magnet candidate, KV_3Sb_5 . *Sci. Adv.* **6**, abb6003 (2020).
- [35] Fujishiro, Y., Kanazawa, N., Kurihara, R., Ishizuka, H., Hori, T., Yasin, F. S., Yu, X., Tsukazaki, A., Ichikawa, M., Kawasaki, M., Nagaosa, N., Tokunaga, M. & Tokura, Y. Giant anomalous Hall effect from spin-chirality scattering in a chiral magnet. *Nat. Commun.* **12**, 317 (2021).
- [36] Uchida, M., Sato, S., Ishizuka, H., Kurihara, R., Nakajima, T., Nakazawa, Y., Ohno, M., Kriener, M., Miyake, A., Ohishi, K., Morikawa, T., Bahramy, M. S., Arima, T., Tokunaga, M., Nagaosa, N. & Kawasaki, M. Above-ordering-temperature large anomalous Hall effect in a triangular-lattice magnetic semiconductor. *Sci. Adv.* **7**, abl5381 (2021).
- [37] Ishizaka, K., Bahramy, M. S., Murakawa, H., Sakano, M., Shimojima, T., Sonobe, T., Koizumi, K., Shin, S., Miyahara, H., Kimura, A., Miyamoto, K., Okuda, T., Namatame, H., Taniguchi, M., Arita, R., Nagaosa, N., Kobayashi, K., Murakami, Y., Kumai, R., Kaneko, Y., Onose, Y. & Tokura, Y. Giant Rashba-type spin splitting in bulk BiTeI. *Nat. Mater.* **10**, 521 (2011).
- [38] Aidoudi, F. H., Aldous, D. W., Goff, R. J., Slawin, A. M. Z., Attfield, J. P., Morris, R. E. & Lightfoot P. An ionothermally prepared $S = 1/2$ vanadium oxyfluoride kagome lattice. *Nat. Chem.* **3**, 801 (2011).
- [39] Clark, L., Orain, J. C., Bert, F., De Vries, M. A., Aidoudi, F. H., Morris, R. E., Lightfoot, P., Lord, J. S., Telling, M. T. F., Bonville, P., Attfield, J. P., Mendels, P. & Harrison, A. Gapless Spin Liquid Ground State in the $S = 1/2$ Vanadium Oxyfluoride Kagome Antiferromagnet $[\text{NH}_4]_2[\text{C}_7\text{H}_4\text{N}][\text{V}_7\text{O}_6\text{F}_8]$. *Phys. Rev. Lett.* **110**, 207208 (2013).
- [40] Okamoto, Y., Nilsen, G. J., Attfield, J. P. & Hiroi, Z. Breathing Pyrochlore Lattice Realized in A-Site Ordered Spinel Oxides $\text{LiGaCr}_4\text{O}_8$ and $\text{LiInCr}_4\text{O}_8$. *Phys. Rev. Lett.* **110**, 097203 (2013).
- [41] Ghosh, P., Iqbal, Y., Müller, T., Ponnaganti, R. T., Thomale, R., Narayanan, R., Reuther, J., Gingras, M. J. P. & Jeschke, H. O. Breathing chromium spinels: a showcase for a variety of pyrochlore Heisenberg Hamiltonians. *npj Quant. Mater.* **4**, 63 (2019).